Available online at www.sciencedirect.com

ScienceDirect

Procedia CIRP 72 (2018) 1433–1438

www.elsevier.com/locate/procedia

51st CIRP Conference on Manufacturing Systems

Investigation of the mechanical properties and cutting performance of cBN-based cutting tools with Cr_3C_2 binder phase.

Kateryna Slipchenko[a,b]*, Igor Petrusha [a], Vladimir Turkevich[a], Jakob Johansson[b], Volodymyr Bushlya[b], Jan-Eric Ståhl[b]

[a]*V.N. Bakul Institute for Superhard Materials of NAS of Ukraine, Kyiv 04074, Ukraine*
[b]*Lund University, Division of Production and Materials Engineering, Lund 221 00, Sweden*

* Corresponding author. Tel.: +380992302421. *E-mail address:* kateryna.slipchenko@iprod.lth.se

Abstract

In order to investigate new materials for metal cutting applications, cubic boron nitride, cutting tools with different amounts of binder phase were sintered in HPHT toroid type apparatus under 7.7 GPa and in temperature range of 1450-2450°C. Initial mixtures of three composition were chosen with 50, 60, 65 vol. % of cBN, 5 vol. % of Al was added to mixture to prevent oxidation. Phase composition, microstructure, elastic properties, hardness, fracture toughness and cutting performance were investigated. The highest value of the mechanical properties and tool life demonstrated samples sintered in temperature range 1850-2150 °C.

Peer-review under responsibility of the scientific committee of the 51st CIRP Conference on Manufacturing Systems.

Keywords: cBN, wear, cutting, HPHR, chromium carbide, sintering, binder

1. Introduction

Cubic boron nitride (cBN) tools are used for machining of difficult to cut steels, cast iron and super alloys. The usage of cBN in metal cutting is steadily increasing and can potentially replace cemented carbides in some applications. When using cBN-based tools for metal cutting, it is oftentimes possible to increase the cutting speed, and thereby productivity, compared to the traditionally used cemented carbide tools and unlike cemented carbides typically containing WC and Co, cBN is to a lesser degree based on critical raw materials [1-3]. The hardness of these tools are second only to polycrystalline diamond tools, PCD. Compared to diamond, cBN is more chemically inert to iron and remains thermally stable at high temperature [4]. The efficiency of cutting tools strongly depends on the microstructural parameters of tool material such as properties of binder phase, distribution of hard cBN grains and interaction between binder phase and cBN.

Commercially, polycrystalline cubic boron nitride (PcBN) is produced by sintering of ultrafine cBN grains with binder phase or sintering additives under high pressure of 4-6 GPa. The most common types of binder phases are metals of group IV in the periodic table and their compounds [5-6]. PcBN materials are divided into two groups low-cBN 40-70 vol. % of cBN, so called BL group, and high-cBN – more than 70 vol. % of cBN, BH group [7].

Costes et al. [8] shown that a low-cBN materials (45-65 vol. %) with a ceramic binder and small grain sizes gives the highest level of tool life during performance testing on Inconel 718. Several wear mechanisms can occurs during cutting. The main of them are abrasion, oxidation, diffusion, adhesion, chemical wear alongside with mechanical failure. Use of ceramic binder such as TiC, AlN, TiCN slow down reactions between cBN and workpiece material, which prolong tool life [9].

A large number of studies have been devoted to the study of interactions and microstructures in systems boron nitride with binders [10-13], and only a few of them have clarified the mechanical properties of obtained composites [14-15]. Morgiel [16] reports about sintering of cBN with Ti (10 wt. %) at 1750

Peer-review under responsibility of the scientific committee of the 51st CIRP Conference on Manufacturing Systems.
10.1016/j.procir.2018.03.180

°C. At this temperature, all titanium reacted with the BN matrix forming TiN and a layer of TiB. Benko et al. [17] report about the formation of TiB_2 and $TiC_{0.8}N_{0.2}$ during thermal treatment of cBN with TiC (1:1 molar ratio at 1400 °C for 2 h), thus confirming thermodynamic calculations. More recently, work of Yang [18] was focused on a study of cBN-based materials with TiC and Al (5-20 wt. %). During sintering at 1350 °C. TiC do not react with cBN but at the same sintering temperature occurs interaction between Al and cBN which resulting in produced AlN and AlB_2. McKie et al. [15] shows the same interaction. For extended duration sintering experiments, 30 min at 1400 °C under 5.8 GPa, performed by Rong et al. [19] reaction was found in the aluminum and cBN and TiN system. The products of these reactions are AlN and TiB. These phases arise around cBN and TiN grains. Formation of a new phases in inter grain space may reinforce the strength of the composites, but excess amount of them also can lead to intergranular fractures. Benko et al. [20] did theoretical and experimental studies of cBN–Cr/Cr_3C_2 systems in 1:1 and 2:1 molar ratios and showed that CrB started forming at 1400 °C. The new phase took place in the intergrain space between cBN and Cr/Cr_3C_2.

2. Experimental details

In the present work cBN micro powders (0.5-2 μm), Al flakes (10 μm) and Cr_3C_2 (1.6 μm) were used as the initial materials. The cBN content in the initial mixtures varies from 50 to 65 vol. %, 5 vol. % of Al were introduced to each mixture and rest volume Cr_3C_2. Before sintering, initial powders were homogenized in a gravitational mixer for 3 h at 120 rpm. Mixing was conducted in isopropyl alcohol medium. Dried powders were compacted into a graphite capsule and annealed in vacuum for 2 h at 600 °C. After thermal treatment, green bodies were placed into the HP assembly for high pressure and high temperature (HPHT) sintering. The experiments were conducted in toroidal type high pressure apparatus with a central hole, 30 mm in diameter (HPA TOR30) under 7.7 GPa pressure. Sintering took place at temperatures between 1450-2450 °C. The samples were subjected to HPHT action for 45 seconds. In order to test material performance, the well-sintered samples were ground to RNGN090300T cutting insert shape. For investigation of the microstructure, the samples were polished using 9 μm and 3 μm diamond suspensions and vibro-polished with silica colloidal suspension.

Densities of sintered compacts (ρ_S) were measured by direct measurements of sizes and mass of samples, and cross-checked with the buoyancy method. X-ray diffraction analysis (STOE STADI MP (CuK_α)) was conducted to determine phase composition of initial powder mixtures and sintered samples. The study of microstructures were done using SEM LEO 1560 microscope with SE2 and InLens detectors. For calculation of elastic modulus, the longitudinal and shear wave sound velocity was measured Olympus 38D Plus pulse-echo tester and from those measurements Young's modulus was derived. For estimation of the hardness and fracture toughness Vickers Hardness Tester THV-30MDX was used. Determination of microhardness was done at 1 kg load, while 5 kg load was used for fracture toughness. Dwell time 15 sec. for both type of measurements. Alicona InfiniteFocus 3-D microscope was used to measure the indenter imprint and crack length in the samples.

Performance testing was conducted on a Torshälla CNC lathe with application of oil emulsion flood coolant. Stainless steel AISI 316L and Vanadis 4E (HRC 60) were chosen for the tests two common representatives of austenitic and martensitic material types. Chemical composition of workpiece materials are given in Table 1.

Table 1 Chemical composition of AISI 316L and Vanadis 4E

Element	AISI 316L	Vanadis 4E
C	0.03%	1.4%
Cr	16-18%	4.7%
Mo	2-3%	3.5%
Mn	2%	0.4%
Si	0.75%	0.4%
V	-	3.7%
Ni	10-14%	-
Fe	Rest Fe	Rest Fe

Cutting conditions corresponded to a finishing operation where feed rate and depth of cut were kept constant at $f = 0.15$ mm/rev and $a_p = 0.3$ mm. Two cutting speeds were used for each workpiece material 150 m/min and 200 m/min for Vanadis 4E; 300 m/min and 500 m/min for AISI 316L. The average flank wear, VB, was measured using Olympus SZX7 stereo microscope.

3. Results and discussion

3.1. X-ray analysis

According to XRD analysis initial powder mixtures for all systems consists of cBN, Cr_3C_2 (tongbarit) and small amounts of aluminum, which was introduced to the mixture to avoid oxidation during HPHT sintering. The aluminum remains not detectable in XRD analysis because of the small amount. Fig. 1 shows the XRD patterns of sample series with 50 vol. % of cBN. Phase composition remains unchangeable during sintering at 1450 °C and 1600 °C.

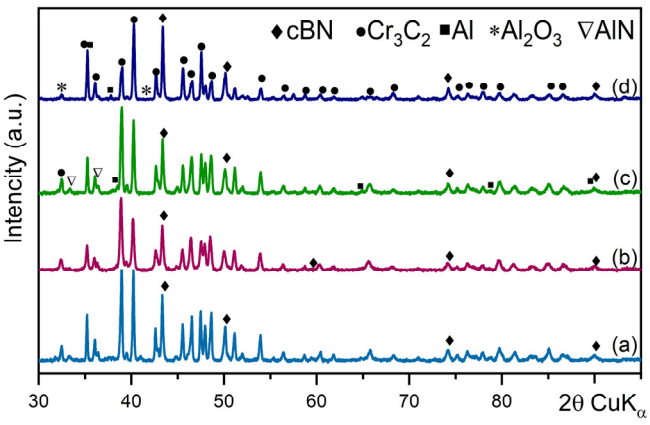

Fig. 1 XRD patterns of cBN-Cr_3C_2-Al system with 50 vol. % cBN sintered at different temperatures (a) 1850 °C; (b) 2150 °C; (c) 2300 °C; (d) 2450 °C.

At sintering temperature 1850 °C traces of pure aluminum and aluminum nitride are observed. When further increasing the sintering temperature, the interaction between aluminum and residual oxygen from the green compact is occurring and as a result peaks that corresponds to Al_2O_3 are observed. In experiments conducted at relatively high temperatures (2300 °C and 2450 °C) precense of pure aluminum or AlN was nor identified. These samples contain only cBN, Cr_3C_2 and Al_2O_3.

In system with 60 vol. % of cBN interaction between components take place at 2150 °C and the phases AlN and CrB_2 are detected in the compound. At 2450 °C the phase composition is complemented by carbon in the form of graphite, see Fig. 2. It is assumed that interaction between components in the mixture occurs according to following reaction:

$$6BN + Cr_3C_2 + 6Al \longrightarrow 3CrB_2 + 6AlN + 2C_{graphite}$$

During experiments at lower temperatures (1600-2000 °C), the phase composition of samples corresponds to the composition of the initial mixture for sintering.

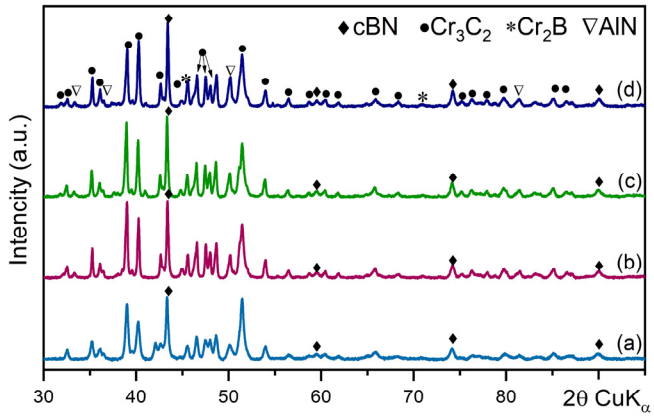

Fig. 2 XRD patterns of cBN-Cr_3C_2-Al system with 60 vol. % cBN sintered at different temperatures (a) 1600 °C; (b) 2150 °C; (c) 2300 °C; (d) 2450 °C.

There is no interaction between the components of the mixture in experiments at 1450 °C and 1600 °C for system with 65 vol. % cBN. Fig. 3 demonstrates that at 2150 °C the interaction between Al and residual oxygen from green compacts occurs.

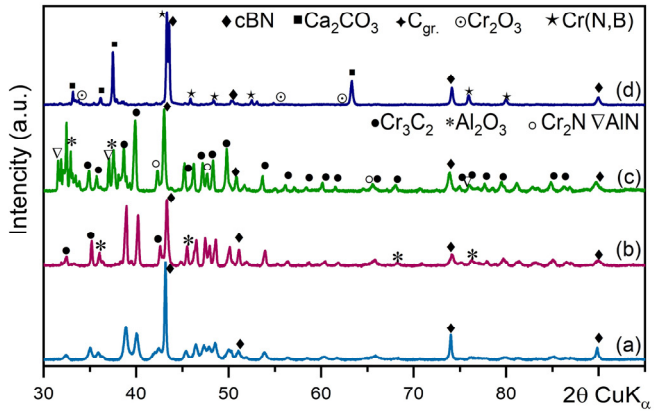

Fig. 3 XRD patterns of cBN-Cr_3C_2-Al system with 65 vol. % cBN sintered at different temperatures (a) 20 °C; (b) 1850 °C; (c) 2300 °C; (d) 2450 °C.

At 2300 °C, Cr_2N and AlN is present but no traces of Al_2O_3 or CrB_2 were evident from XRD analysis. The failure of the graphite HPHT capsule took place at 2450 °C, resulting in infiltration of $CaCO_3$ from the high-pressure cell assembly into the green bodies.

3.2. SEM

Typical microstructures of sintered PcBN materials are shown in Fig. 4. It is clearly visible that the binder phase in the light grey areas homogeneously surrounds cBN grains, shown as the dark grey areas.

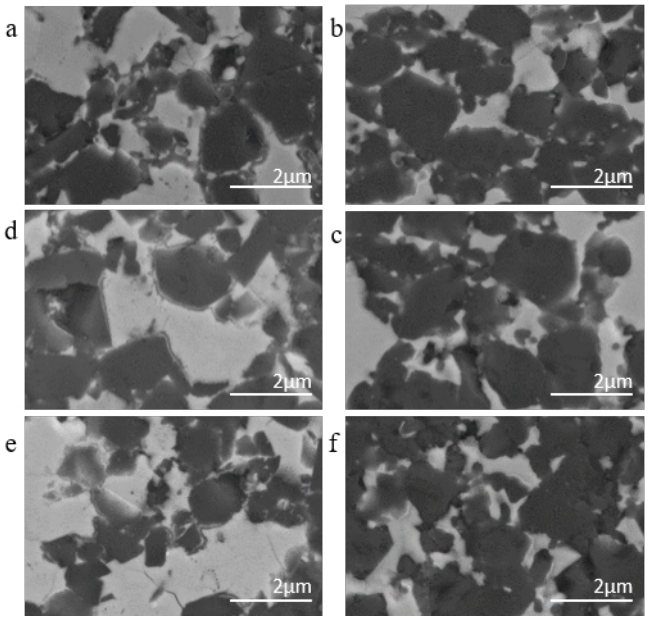

Fig. 4 SEM microstructures of the samples in system with 50 vol. % of cBN at 1850 °C (a), 2300 °C (b); 60 vol. % of cBN at 1850 °C (c), 2300 °C (d); 65 vol. % of cBN at 1850 °C (e) and 2300 °C (f) under a pressure of 7.7 GPa for 45 s.

At sintering temperature 1850 °C in all system cBN grains has relatively sharp edges, which additionally confirms the absence of chemical interactions involving cBN, see Fig. 4 a, c, e. At the presence of interactions between the components in a mixture, the boundaries of cBN grains change their morphology to a rounded ones. This effect is noticeable in systems with 50 and 60 vol. % of cBN, see Fig. 4 b, d.

3.3. Mechanical properties

Fig. 5 shows densities of composites after HPHT sintering process. The density of samples that were subject only to pressure without heating are 20-30% lower than in samples sintered at high temperatures. Application of HPHT leads to increase of density at temperature range of 1450-1850 °C in all investigated systems.

Sintering in temperature range of 2000-2450 °C does not have large influence on a density. Thus, it is possible that a certain limit of compaction that corresponds to the densities of initial materials was achieved. High level of densification during HTHP sintering positively effect on mechanical properties of the materials.

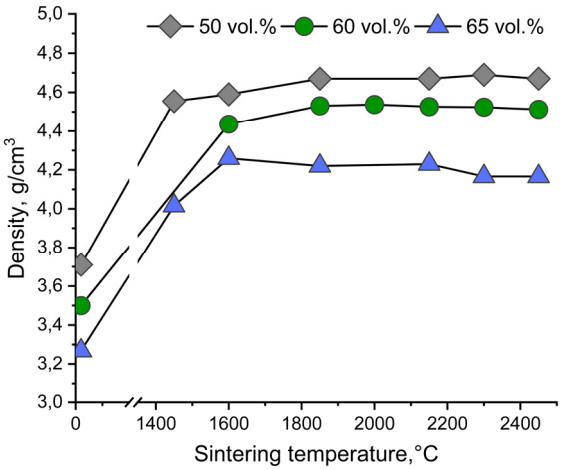

Fig. 5 Density of cBN-based materials versus sintering temperature.

Young's modulus in all groups of samples has tendency to increase with higher sintering temperature up to 1850 °C (Fig. 6). Also noteworthy is that in all groups this parameter changes in two steps, first increasing with increasing sintering temperature and after reaching of some temperature which is specified per amount of cBN, Young's modulus first decreases until a sintering temperatures where the modulus increases again.

In systems with 60 and 65 vol. % of cBN this changes occurs at 2150 °C, but the system with 60 vol. % a more distinct step is visible. Such change in the systems is driven by the interactions of components in the material under HPHT conditions.

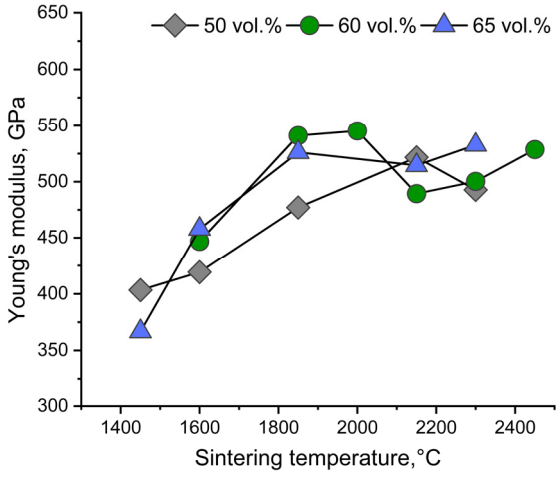

Fig. 6 Young's modulus of cBN-based materials versus sintering temperature.

It is possible to identify a few general trends of microhardness changes in studied samples shown in Fig. 7. Firstly, in all series, the microhardness is increasing in the temperature range 1400 - 1850 °C. In this temperature range no interaction between components of the mixture occurs. Secondary, microhardness in systems with 50 and 60 vol. % cBN continue to increase at higher temperatures, while in system with 65 vol. % it start decreasing. Maximum values of microhardness at system with 50 and 65 vol. % is found in samples sintered at 2150 °C and 2000 °C respectively. Thirdly, samples from all systems sintered at 2300 °C have approximately the same value of microhardness, which can be explained by the completeness of the interaction of the components, i.e. formation of chromium diboride and aluminum nitride.

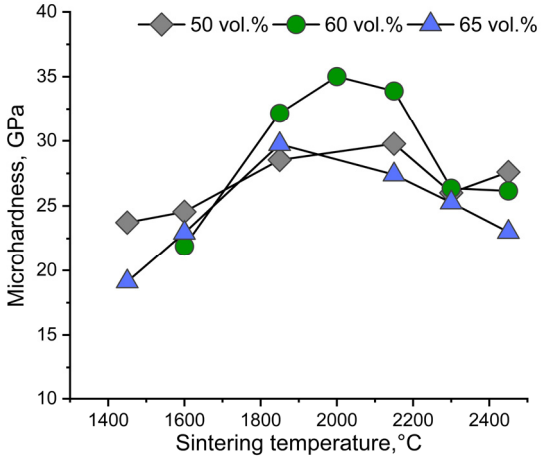

Fig. 7 Microhardness of cBN-based materials versus sintering temperature.

Fig. 8 shows that fracture toughness of sintered samples in all groups slightly increase with application of higher temperatures. Samples sintered at 1600 °C have relatively equal values of fracture toughness.

Meanwhile samples that were sintered under the same HPHT condition have relatively close values of fracture toughness. It can be seen that system with 50 vol. % and 65 vol. % of cBN reaches their maximal fracture toughness at 2150 °C and 2300 °C respectively and above it the values decrease.

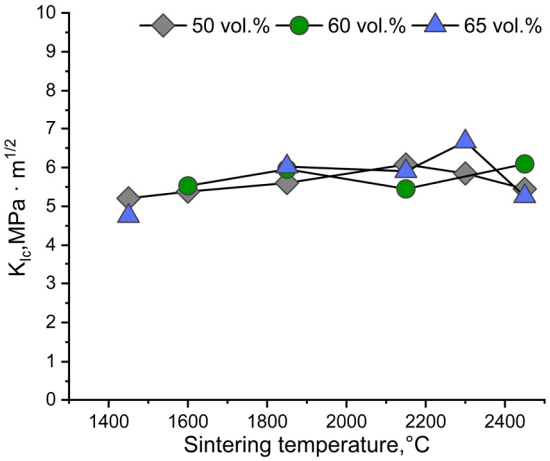

Fig. 8 Fracture toughness of cBN-based materials versus sintering temperature.

3.4. Performance testing

Fig. 9 shows the values of flank wear on the tested tools which developed after 30 sec when turning stainless steel AISI 316L. Samples sintered at 2450 °C were not tested since they fragmented during the sintering process and therefore it was not possible to achieve the desired tool geometry. The highest tool wear is typically found for samples sintered at 1450-1600 °C were the densification of the material was not completed and the microhardness is lower than in other samples.

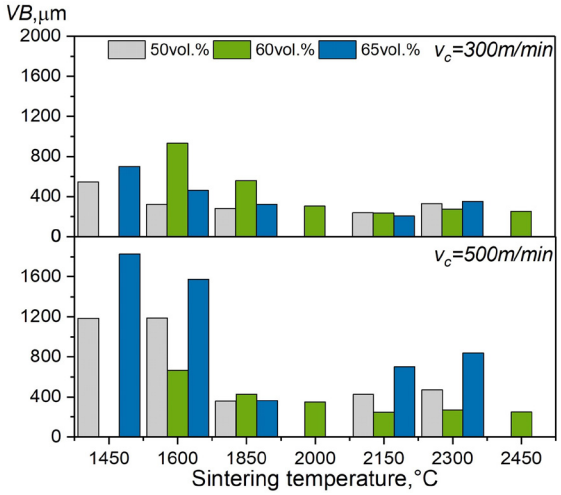

Fig. 9 Tool wear development when machining AISI 316L.

Samples in the system with 50 vol. % of cBN are more wear resistant when machining at v_c = 300 m/min. According to findings of Bushlya et al. [2-3] the main wear mechanisms are chemical and diffusional wear and 50 vol. % of binder phase protect cBN phase. When increasing the cutting speed to 500 m/min tool wear rapidly increases (Fig. 10 a, b), probably due to increased temperature in the cutting zone.

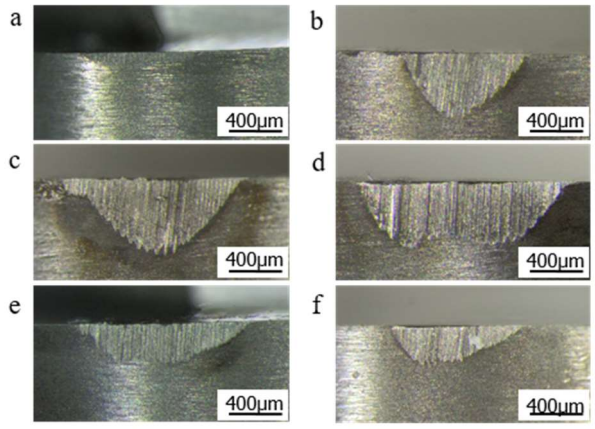

Fig. 10 Optical micrographs of the wear on samples sintered at 1850 °C after turning on 316L in system with 50 vol. % of cBN v_c = 300 m/min (a), v_c=500m/min (b); 60 vol. % of cBN v_c = 300 m/min (c), v_c = 500 m/min (d); 65 vol. % of cBN v_c = 300 m/min (e), v_c = 500 m/min (f).

Roughly the same degree of tool wear is found in the system with 60 vol. % of cBN on both cutting speeds (Fig. 10 c, d). For system with 65 vol. % of cBN, the sample sintered at 1850 °C shown the same level of VB on both tests (Fig. 10 e, f) and therefore cutting speed do not appear to have a significant impact on the tool wear. In the experiments on Vanadis 4E, the system with 50 vol. % of cBN showed the highest rate of tool wear (Fig. 11). The most favourable results were obtained while machining with samples from system with 60 vol. % of cBN in both applied speeds. The test results in the system with 65 are close to the system with 60 vol. % of cBN.

Comparing the optical images of flank wear (Fig. 12 a, c, e) it can be hypothesized that in case cutting speed 150m/min the wear mechanism is dominated by both chemical and abrasive wear mechanisms. With the increase of cutting speed, both of these wear mechanism are accompanied by active mechanical degradation and breakage of cutting tools (Fig. 12 b, d, f).

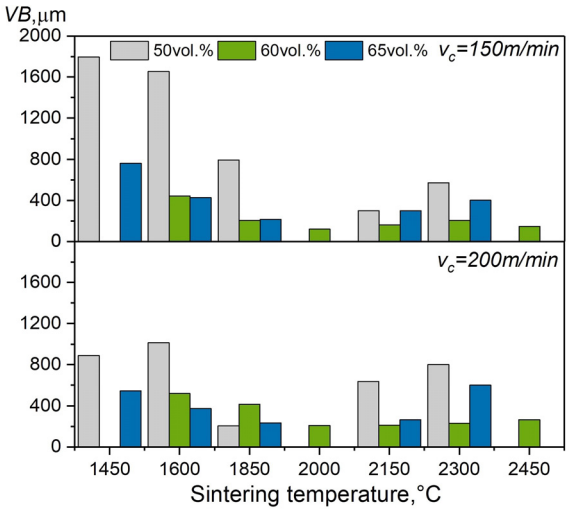

Fig. 11 Tool wear development when machining Vanadis 4E.

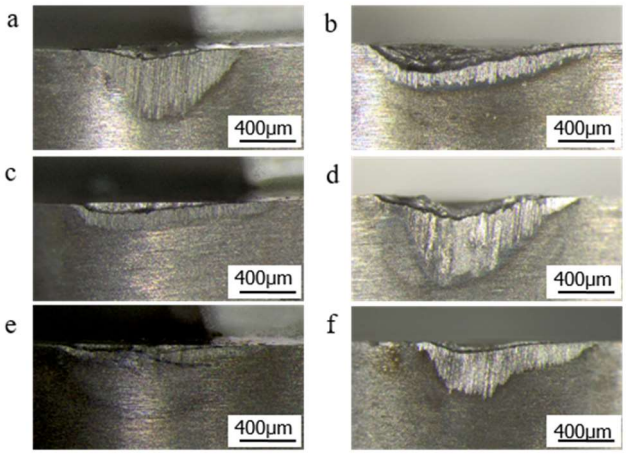

Fig. 12 Optical micrographs of the tool wear on samples sintered at 1850 °C after turning on Vanadis 4E in system with 50 vol. % of cBN v_c = 150 m/min (a), v_c = 200 m/min (b); 60 vol. % of cBN v_c = 150 m/min (c), v_c = 200 m/min (d); 65 vol. % of cBN v_c = 150 m/min (e), v_c = 200 m/min (f).

From statistical analysis, it was found that dominant influence on tool wear is found for the sintering temperature and microhardness of the sintered materials.

It should be noted that despite the observed superior mechanical properties of the obtained PcBN materials in the designated systems their performance in machining operations of AISI 316L and Vanadis 4E workpiece materials was significantly less than the acceptable industrial standard. This is most likely related to the reduced chemical stability and higher diffusional wear of the binder systems compared to the commercial TiC or Ti(C,N) binders.

Conclusions

In this study mixtures of cBN, Cr_3C_2 and Al were used to fabricate PcBN cutting materials at wide range of compositions and temperatures under 7.7 GPa sintering pressure. Phase

composition, microstructures and mechanical properties of three groups of samples were studied and compared.

- During HPHT sintering at temperatures above 1850 °C Al and Cr_3C_2 interact with cBN and/or O_2.
- Binder phase homogeneously surrounded cBN grains. Increasing the sintering temperature promoted the chemical interaction which has influenced cBN grain morphology.
- System with 60 vol. % of cBN has the highest microhardness value. The material hardness, alongside with other measured mechanical properties, achieved the highest values between 1850-2150 °C which can be considered as an optimum sintering temperature.
- The increase of sintering temperature has almost no effect on the fracture toughness of the samples. It remains within the range of 5 - 6.5 $MPa \cdot m^{1/2}$.
- The highest wear resistance during machining of AISI 316L and Vanadis 4E was found for the system with 60 vol. % of cBN sintered at temperature between 1850-2150 °C.

Acknowledgements

This research was supported by European Union's Horizon 2020 Research and Innovation Programme under Flintstone2020 project (grant agreement No. 689279) and Visby Scholarship by the Swedish Institute (grant number 02757/2016). It is also a part of the Sustainable Production Initiative cooperation between Lund University and Chalmers University of Technology. The authors also would like to express their gratitude to Daniel Johari for help with performance testing.

References

[1] EC-European Commission. (2010). Critical raw materials for the EU. *Report of the ad-hoc working group on defining critical raw materials. Brussels.*

[2] Bushlya, V., Zhou, J., & Ståhl, J. E. (2012). Effect of cutting conditions on machinability of superalloy Inconel 718 during high speed turning with coated and uncoated PCBN tools. *Procedia CIRP, 3*, 370-375.

[3] Bushlya, V., Zhou, J., Avdovic, P., & Ståhl, J. E. (2013). Performance and wear mechanisms of whisker-reinforced alumina, coated and uncoated PCBN tools when high-speed turning aged Inconel 718. *The International Journal of Advanced Manufacturing Technology,* 1-9.

[4] Wentorf, R. H., DeVries, R. C., & Bundy, F. P. (1980). Sintered superhard materials. *Science*, 208(4446), 873-880.

[5] Venezar, N. P. (1986). Polucenie i Primienienie Sverhtverdych Materialov. *ISM USSR, Kiev.*

[6] Benko, E., Wyczesany, A., & Barr, T. L. (2000). CBN-metal/metal nitride composites. *Ceramics international*, *26*(6), 639-644.

[7] ISO 1832:2017. Indexable inserts for cutting tools–Designation.

[8] Costes, J. P., Guillet, Y., Poulachon, G., & Dessoly, M. (2007). Tool-life and wear mechanisms of CBN tools in machining of Inconel 718. *International Journal of Machine Tools and Manufacture*, 47(7), 1081-1087.

[9] Bushlya, V. M., Gutnichenko, O. A., Zhou, J. M., Ståhl, J. E., & Gunnarsson, S. (2014). Tool wear and tool life of PCBN, binderless cBN and wBN-cBN tools in continuous finish hard turning of cold work tool steel. *Journal of Superhard Materials, 36*(1), 49-60.

[10] Kim, S. G., Jon, G. I., & Im, S. J. (2016). Experimental study on the influence of binders on plastic deformation during sintering of cubic boron nitride powder under high pressure and high temperature. *arXiv preprint arXiv:1604.08499*.

[11] Chiou, S. Y., Ou, S. F., Jang, Y. G., & Ou, K. L. (2013). Research on CBN/TiC composites Part1: Effects of the cBN content and sintering process on the hardness and transverse rupture strength. *Ceramics International*, 39(6), 7205-7210.

[12] Angseryd, J., Liu, F., & Andrén, H. O. (2015). Nanostructure of a cubic BN cutting tool material. *International Journal of Refractory Metals and Hard Materials, 49*, 283-287.

[13] Lindgren, K. E., Kauppi, A., & Falk, L. K. L. (2017). Development of matrix microstructure in polycrystalline cubic boron nitride ceramics. *Journal of the European Ceramic Society, 37*(9), 3017-3026.

[14] Harris, T. K., Brookes, E. J., & Taylor, C. J. (2004). The effect of temperature on the hardness of polycrystalline cubic boron nitride cutting tool materials. *International Journal of Refractory Metals and Hard Materials, 22*(2), 105-110.

[15] McKie, A., Winzer, J., Sigalas, I., Herrmann, M., Weiler, L., Rödel, J., & Can, N. (2011). Mechanical properties of cBN–Al composite materials. *Ceramics International, 37(*1), 1-8.

[16] Morgiel, J., & Benko, E. (1995). Microstructure of boron nitride sintered with titanium. *Materials Letters, 25*(1-2), 49-52.

[17] Benko, E., Barr, T. L., Hardcastle, S., Hoppe, E., Bernasik, A., & Morgiel, J. (2001). XPS study of the cBN–TiC system. *Ceramics International, 27*(6), 637-643.

[18] Yang, L., Yue, Z., Gong, J., Zhao, X., & Chu, X. (2017). Compositions, mechanical properties and microstructures of cBN-based composites sintered with Al or TiC. *Advances in Applied Ceramics*, 1-6.

[19] Rong, X. Z., Tsurumi, T., Fukunaga, O., & Yano, T. (2002). High-pressure sintering of cBN-TiN-Al composite for cutting tool application. *Diamond and Related Materials, 11*(2), 280-286.

[20] Benko, E., Wyczesany, A., Bernasik, A., Barr, T. L., & Hoope, E. (2000). CBN–Cr/Cr3C2 composite materials: chemical equilibria, XPS investigations. *Ceramics International, 26*(5), 545-550.